



**HAL**  
open science

## ADRC based speed control applied to a micro-hydropower plant

Baoling Guo, Seddik Bacha, Mazen Alamir

► **To cite this version:**

Baoling Guo, Seddik Bacha, Mazen Alamir. ADRC based speed control applied to a micro-hydropower plant. JCGE 2017 - 14ème Conférence des Jeunes Chercheurs en Génie Électrique, May 2017, Arras, France. hal-01533679

**HAL Id: hal-01533679**

**<https://hal.science/hal-01533679>**

Submitted on 20 Jun 2017

**HAL** is a multi-disciplinary open access archive for the deposit and dissemination of scientific research documents, whether they are published or not. The documents may come from teaching and research institutions in France or abroad, or from public or private research centers.

L'archive ouverte pluridisciplinaire **HAL**, est destinée au dépôt et à la diffusion de documents scientifiques de niveau recherche, publiés ou non, émanant des établissements d'enseignement et de recherche français ou étrangers, des laboratoires publics ou privés.

# ADRC based speed control applied to a micro-hydropower plant

Baoling GUO<sup>1</sup>, Seddik BACHA<sup>1</sup>, Mazen ALAMIR<sup>2</sup>

<sup>1</sup> Univ. Grenoble Alpes, CNRS, Grenoble INP\*, G2Elab, F-38000 Grenoble, France

<sup>2</sup> Univ. Grenoble Alpes, CNRS, Grenoble INP\*, GIPSA lab, F-38400 Saint Martin D'Hères, France

*baoling.guo@g2elab.grenoble-inp.fr, Seddik.Bacha@univ-grenoble-alpes.fr, mazen.alamir@gipsa-lab.grenoble-inp.fr*

**ABSTRACT** – Micro-hydropower brings a significant contribution to the renewable energy section due to its huge potential through the world. Hydraulic turbine efficiency is sensitive to the water flow rates and the rotational speed variations, so the variable-speed operation is required to ensure the maximum efficiency in a micro-hydropower generation system (MHPGS). To realize the maximum power point tracking (MPPT), the hydro turbine rotation speed changes with the water flow rates variations, this proposes higher speed tracking demands. Moreover, a MHPGS is a typical complex nonlinear system disturbed by numerous uncertainties. Active Disturbance Rejection Control (ADRC) technology is a novel approach which can estimate and compensate the influences of internal and external disturbances in real time, which has realized excellent control performance in various fields. To improve the speed tracking performance, an ADRC based speed control is proposed in this paper. Simulation and experiment results have proved that the proposed approach can track the speed variations efficiently.

**KEY WORDS** – MHPGS, PMSG, variable speed, ADRC, speed control, disturbance.

## 1. Introduction

Small hydropower or micro-hydropower has a huge potential in the renewable energy section [1-4]. On a global scale, the small hydropower represents approximately 1.9 percent of the global power capacity, 7 percent share in the total renewable energy capacity and ranks fifth in the global share of renewable energy [1]. This paper focuses on micro-hydropower, the capacity of the micro-hydropower plant ranges from 20 KW to 500 KW or even smaller depending on the local definitions [2] [3].

"Run off river" is the first choice for a large majority of micro-hydropower plants with low heads and high water flow rates. The semi-Kaplan and propeller hydro turbines become most attractive for MHPGSs due to their high efficiency in such conditions [2-4]. The efficiency of a Semi-Kaplan turbine is very sensitive to water flow rates and rotational speed variations, hence, a variable-speed MHPGS, which can operate over a large speed range, has a great potential in ensuring the MPPT [3]. The variable speed operation is usually integrated into the power system through Power Electronics (PE) [5], which can improve the power quality, provide the reactive power control or the voltage regulation, and also have a Low Voltage Ride Through capability [6]. A unit of the direct drive PMSG has been widely equipped for MHPGSs [2-5]. It has double back-to-back PWM converters connected between the stator and the grid, which totally decouples the generator from the grid. Hence, grid disturbances have no direct effects on the generator, further reducing the current and torque variations.

To realize the MPPT in a variable speed MHPGS, the hydro turbine rotation speed changes with the water flow rates variations, which proposes higher speed tracking demands, meanwhile, a variable speed system MHPGS is a typical nonlinear system disturbed by large uncertainties from the internal and the external, which greatly influence the speed control performance [2-7] [13-15]. Recently, large efforts are devoted to improving the speed control performance of a PMSG [8] [9], the ADRC based speed control stands out among various algorithms [13-15]. ADRC is categorized into the nonlinear control [10-12]. A full account of the ADRC paradigm is provided in [10]. ADRC is based on a fact that many dynamic systems, linear or nonlinear, under some conditions can be transformed into the canonical form of cascade integrators via a feedback [11]. The feedback includes the connection information or the uncertain disturbances in the control system. Extended State Observer (ESO) can estimate the unknown disturbance in real time and then compensate the influences in the closed-loop dynamics, which realize great robustness in dealing with disturbances [11].

Due to its remarkable abilities in dealing with disturbances, ADRC was widely introduced into the speed control of AC servo control systems [13-15]. Paper [13] replaces the PI controller with the first-order ADRC in the PMSM speed control loop. The control performance depends largely on the ESO estimation precision. To decrease the estimation burden and increase its accuracy, partial disturbances are identified in [14]. Moreover, a first-order ADRC based speed controller neglects the dynamics of the current loop; to avoid this simplification, a second-order ADRC based speed control design is proposed in [15].

In this paper, the variable speed MHPGS is based on the form of "Run off river"; meanwhile, to improve the global efficiency, the semi-Kaplan hydro turbine and the direct drive PMSG structure implemented. Large applications prove the advantages of the ADRC, to improve the speed tracking performance of the variable speed MHPGS, an ADRC based speed control is proposed. The paper is structured as follows. Section 2 describes the model of a variable speed MHPGS and its global control objectives. In section 3, to improve the speed tracking performance of the MHPGS, an ADRC based speed control approach is proposed. Simulations and experiments are conducted to prove the effectiveness of the proposed strategy in section 4. Conclusions are indicated in the last section.

## 2. Mathematical model of a micro-hydro power plant

The hydraulic power directly depends on the water head and water flow rate as

$$P_h = \rho \cdot g \cdot H \cdot Q_w \quad (1)$$

Hydraulic turbine efficiency is considered, as it greatly affects the net output mechanical power by

$$P_{mech} = \eta \cdot \rho \cdot g \cdot H \cdot Q_w \quad (2)$$

where  $P_{mech}$  (Watts) is the mechanical power produced on the turbine shaft,  $\eta$  is the hydraulic turbine efficiency,  $\rho$  ( $\text{kg/m}^3$ ) the volume density of water,  $g$  the acceleration due to gravity ( $\text{m/s}^2$ ),  $Q_w$  ( $\text{m}^3/\text{s}$ ) the water flow rate passing through the turbine, and  $H$  (m) is the net head of water across the turbine.

For a fixed head, the steady-state power efficiency of the considered hydraulic turbine has been experimentally described in [4]. The efficiency of the turbine can be approximated mathematically by,

$$\begin{cases} \eta(\lambda, Q_w) = \frac{1}{2} \left[ \left( \frac{90}{\lambda_i} + Q_w + 0.78 \right) \cdot \exp\left(-\frac{50}{\lambda_i}\right) \right] \cdot 3.33 \cdot Q_w \\ \lambda_i = [1 / (\lambda + 0.089) - 0.035]^{-1}, \quad \lambda = R \cdot A \cdot \omega / Q_w \end{cases} \quad (3)$$

where  $R$  (m) the radius of the hydraulic turbine,  $A$  ( $\text{m}^2$ ) the area swept by rotor blades,  $\Omega$  (rad/s) the rotational speed.

The power efficiency curves described by (3) are presented in Figure 1 (a) and the MPPT curves are shown in Figure 1(b). With water flow rates changing, the speed loop will track an optimal rotation speed to make the system absorb the maximum power in a well-controlled MHPGS.

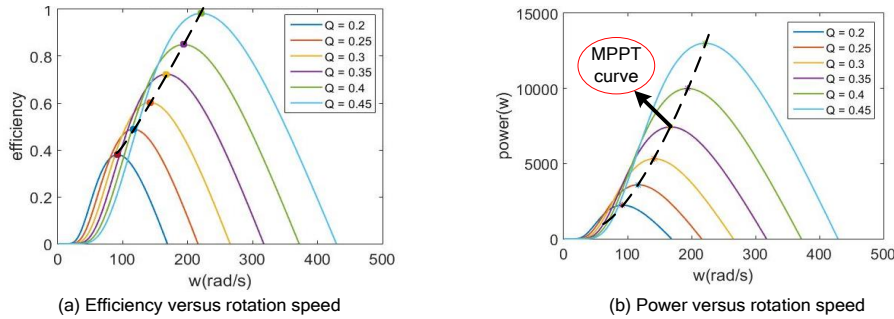


Figure 1 : Efficiency and maximum power tracking curves of a micro-hydro power plant

## 3. Mathematical model of a PMSG

The mathematical model of a three-phase PMSG in  $dq$  coordinate [2] is described as

$$\begin{cases} v_d = L_d \frac{di_d}{dt} + R_s i_d - \omega_e L_q i_q \\ v_q = L_q \frac{di_q}{dt} + R_s i_q + \omega_e (L_d i_d + \psi_f) \end{cases} \quad (4)$$

where  $v_d$  and  $v_q$  are the stator voltage q axis and d axis vector,  $i_q$  and  $i_d$  are the stator current q axis and d axis vector,  $R_s$  is the stator winding resistance,  $L_d$ ,  $L_q$  are the inductance of stator winding q axis and d axis components,  $\psi_f$  the permanent magnet flux vector,  $\omega_e$  is the electrical rotation speed,  $P_n$  is the number of pole pairs.

Electromagnetic torque  $T_e$  in the  $dq$  coordinate system is given as

$$T_e = \frac{3}{2} p_n (\psi_f i_q + (L_d - L_q) i_d i_d) \quad (5)$$

If  $L_d = L_q$  or make  $i_d = 0$ , then  $T_e$  can be modified as below

$$T_e = \frac{3}{2} p_n \psi_f i_q \quad (6)$$

A mechanical dynamic connection between the mechanical torque  $T_{mec}$  and  $T_e$  is built as

$$J \frac{d\omega}{dt} = T_e - T_{mec} - B\omega \quad (7)$$

## 4. ADRC based rotation speed control

A variable speed system MHPGS is a typical complex nonlinear system disturbed by many uncertainties. Firstly, there are cases where the turbine operates at unstable regions, usually being avoided, which results in large fluctuations; besides, the PE itself is also a nonlinear system with unpredictable disturbances. ADRC is a relatively novel approach which can estimate all internal and external disturbances, and then compensate the influences in the closed loop in real time. Combined with the special nonlinear feedback structure, it realizes high performance in many fields [12].

### 4.1 ADRC standard model formulation

In [10], it is pointed out an important fact about many systems with feedback, no matter dynamic system, linear or non-linear, under some conditions can be transformed into the canonical of cascade integrators via the feedback, the boundary between the linear and the nonlinear can be broken by the control input signal. The advantage it brings is that a complete mathematical model of the plant is not obligatory.

A first-order canonical form of cascaded integrators is represented with

$$\begin{cases} \dot{x} = f(x, w) + bu = f_0(\hat{x}, \hat{w}) + f_1(x, w) + bu \\ y = x \end{cases} \quad (8)$$

where  $f(\cdot) = f_0(\hat{x}, \hat{w}) + f_1(x, w)$  the total disturbances of the system,  $f_0(\hat{x}, \hat{w})$  the known disturbances, and  $f_1(x, w)$  the unknown disturbances, respectively,  $x$  is the state variable,  $w$  is the uncertain external disturbances,  $u$  is the control input,  $y$  is the output.

Before applications of the ADRC paradigm, the key point is to reformulate the practical control issue to be the same form as (8), namely, a formula between the control signal  $u$  and the output  $y$ . A first-order formula between the control signal  $i_q$  and the output  $\omega$  is rewritten as

$$\dot{\omega} = \frac{1.5P_n\psi_f i_q}{J} - \frac{T_{mec}}{J} - \frac{B\omega}{J} = f_0(\hat{\omega}, \hat{T}_{mec}) + bi_q \quad \text{with } b = \frac{1.5P_n\psi_f}{J} \quad (9)$$

To highlight, the larger the total disturbance is, the less accurate the ESO estimation is [18-20], so the disturbance definition is crucial for the ADRC design.

**Table 1. Different disturbance definition strategies**

| Disturbance definition   | Total disturbance estimated   |
|--|---|
| $f_{case1}(\cdot) = f_1(\omega, T_{mec}) = -\frac{T_{mec}}{J} - \frac{B}{J}\omega$                         | $a_{case1}(t) = -\frac{T_{mec}}{J} - \frac{B\omega}{J} + (b - b_0)i_q$  |
| $f_{case2}(\cdot) = f_0(\hat{\omega}) + f_1(T_{mec}) = -\frac{B}{J}\hat{\omega} + (-\frac{T_{mec}}{J})$    | $a_{case2}(t) = -\frac{T_{mec}}{J} - (\frac{B\omega}{J} - \frac{B\hat{\omega}}{J}) + (b - b_0)i_q$                            |
| $f_{case3}(\cdot) = f_0(\hat{\omega}, \hat{T}_{mec}) = -\frac{B}{J}\hat{\omega} - \frac{\hat{T}_{mec}}{J}$ | $a_{case3}(t) = -\frac{T_{mec}}{J} - \frac{B\omega}{J} - (-\frac{B}{J}\hat{\omega} - \frac{\hat{T}_{mec}}{J}) + (b - b_0)i_q$ |

Firstly, it can treat  $-\frac{T_{mec}}{J} - \frac{B}{J}\hat{\omega}$  as the total disturbances as the case 1 shown in table I, which is easy to be implemented, however, due to the speed changes or sudden torque fluctuations, the ESO estimation accuracy will be affected. In [13], to mitigate the effect of a speed change,  $-\frac{B}{J}\hat{\omega}$  is treated as known disturbances as the case 2 shown in table I, where  $\hat{\omega}$  can get from the estimation result of an ESO. In case 3, the load torque is identified in [14], let  $b =$

$b_0 = \frac{1.5P_n\psi_f}{J}$ , the disturbances estimated by the ESO is nearly zero, which helps reduce the ESO estimation burden; correspondingly, the speed tracking performance is improved.

In this paper, the friction factor and its inertia are assumed constant, even in practice; they have small variations due to aging factor, and the friction factor is also non-constant in operation. The uncertainties can be treated as dynamics, which can be estimated by the ESO in real time.

## 4.2 Design of ADRC based speed control

A standard ADRC paradigm has 3 key modules [10]: 1) a transient profile generator and a noise-tolerant tracking differentiator; 2) a nonlinear control feedback; 3) ESO for the total disturbance estimation and rejection. In applications, to avoid the set-point jump, a transient profile is constructed, but it sacrifices the dynamic response time, usually, it can be neglected in a first-order system. Finally, the diagram of an ADRC based speed control is shown in Figure 2.

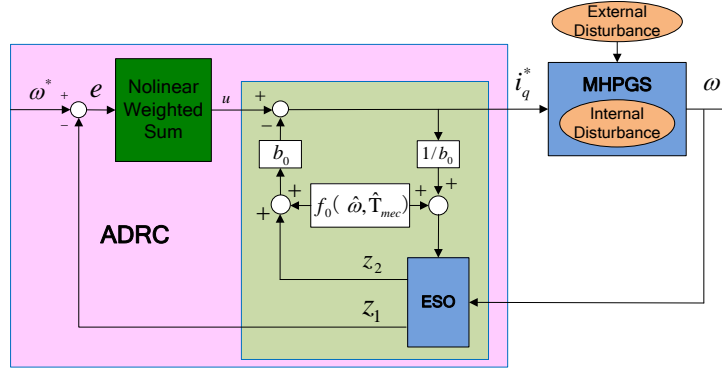


Figure 2 : Diagram of ADRC based speed control

### 4.2.1 Nonlinear control law

A nonlinear law of (10) is applied to make the feedback control and the ESO more efficient, which has been proved in large implementations [10].

$$fal(\varepsilon, \alpha, \delta) = \begin{cases} |\varepsilon|^\alpha \operatorname{sgn}(\varepsilon), & |\varepsilon| > \delta \\ \varepsilon / \delta^{1-\alpha}, & |\varepsilon| \leq \delta \end{cases} \quad (10)$$

The nonlinear law depends on the parameters  $\alpha$  and  $\delta$ [10]. If  $0 < \alpha < 1$ , (10) has a characteristic of ‘large error, small gain; small error, large gain’ as shown in Figure 3(a), which makes the tracking error reach zero faster. Besides, the feedback efficiency varies with different  $\delta$  values as shown in Figure 3(b).

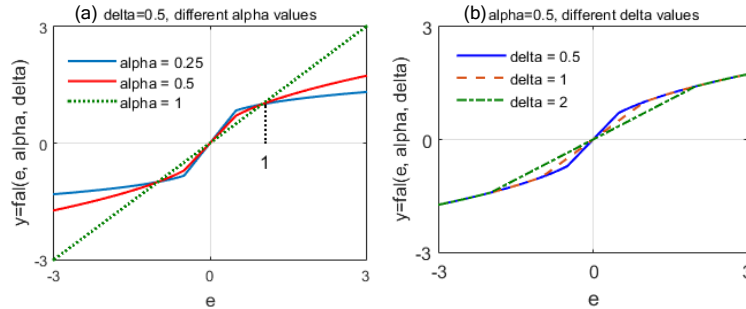


Figure 3 : Diagram of the nonlinear law

### 4.2.2 ESO (Extended State Observer)

An ESO can estimate both the states and the disturbances simultaneously. The mathematical model is described as

$$\begin{cases} \dot{\varepsilon}_1 = z_1 - \omega \\ \dot{z}_1 = z_2 - \beta_1 fal(\varepsilon_1, \alpha_1, \delta_1) - b i_q \\ \dot{z}_2 = -\beta_2 fal(\varepsilon_1, \alpha_2, \delta_1) \end{cases} \quad (11)$$

where  $z_1, z_2$  is the estimation of  $\omega$  and the total disturbances, respectively,  $\beta_1, \beta_2$  are the observer gains.

### 4.2.3 Nonlinear weighted sum

Finally, the nonlinear weighted sum can be represented with (12), which makes the controller more efficient.

$$\begin{cases} e_1 = \omega^* - z_1 \\ i_{q0} = \beta_0 \text{fal}(e_1, \alpha_0, \delta_0) \\ i_q = i_{q0} - z_2 / b \end{cases} \quad (12)$$

$\beta_1$  is the proportional gain. Tuning principles of parameters  $\beta_0, \beta_1, \beta_2, \alpha_0, \alpha_1, \alpha_2, \delta_0, \delta_1$  are fully discussed in [10] [16].

## 5. Simulation and experiment results

### 5.1 Simulation results

To verify the speed tracking performance of the proposed ADRC based control approach, simulation studies are conducted in the Matlab/Simulink. The scheme of ADRC based speed control is shown in Figure 4. The output of an ADRC works as the q axis current control loop reference, which is treated as the plant input, d axis current reference is set zero to control the reactive power to be zero, PI controllers are chosen for the inner current loops.

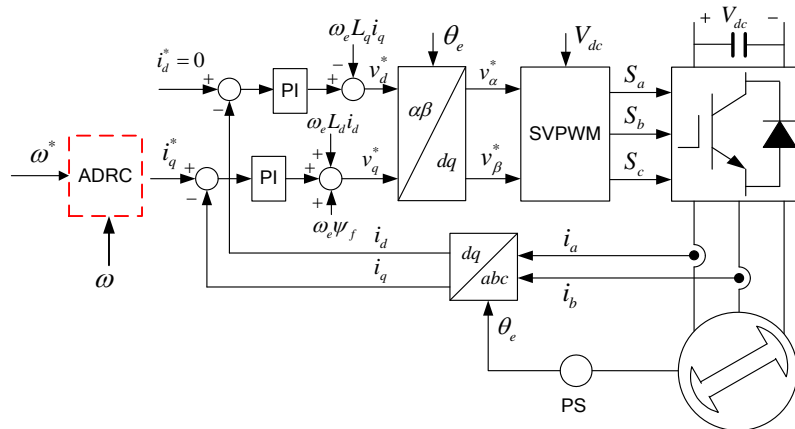


Figure 4 : ADRC based speed control diagram of a MGHP

Parameters of the PMSG used in simulations are shown in table 2.

Table 1. Parameters of PMSG

| Parameters          | Value         | Parameters           | Value                    |
|---------------------|---------------|----------------------|--------------------------|
| Armature resistance | 0.17 $\Omega$ | Pole pairs number    | 4                        |
| d-axis inductance   | 0.0017 H      | Total inertia        | 0.0048 $Kg \cdot m^2$    |
| q-axis inductance   | 0.0019 H      | Friction coefficient | 0.01 $N \cdot m \cdot s$ |
| Magnet flux vector  | 0.11 Wb       | Switch frequency     | 10 KHz                   |

Firstly, to verify the speed tracking performance of different disturbance definition strategies, 3 cases in table 1 are conducted in the simulation. A constant reference speed is applied and a load torque disturbance happens at  $t=0.1s$ . In case 3, the total disturbance estimated by ESO is nearly zero as shown in Figure 5(a), which performs best in three cases as shown in Figure 5(b). Simulation results have proved the effectiveness of the disturbance compensation. In the following simulation, only case 3 is considered.

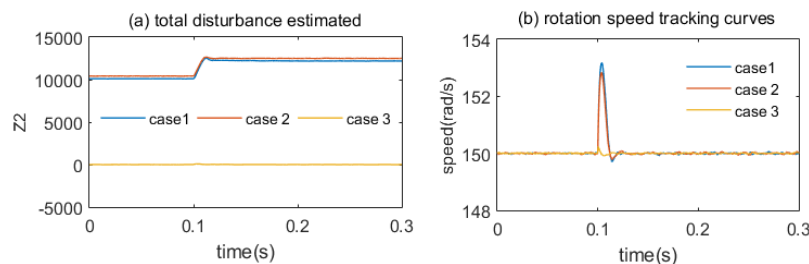
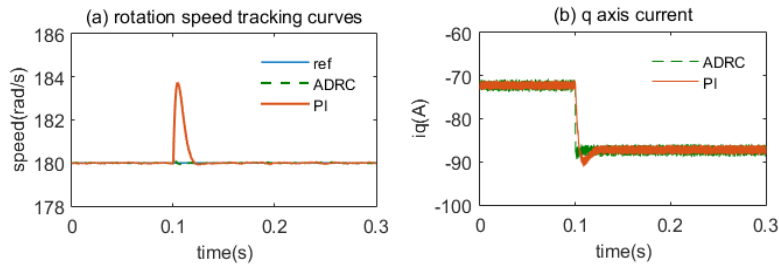


Figure 5 : Disturbances estimated and speed dynamic response

Secondly, the comparative simulations between the PI and the ADRC are conducted.

Case1: An ADRC based speed control strategy for PMSM is simulated with  $\omega^* = 180\text{rad/s}$ . A load torque of  $-50\text{N.m}$  is initially applied, and then decreased to  $-60\text{N.m}$  at  $0.1s$ . Compared with the PI controller, the speed tracking process of

the ADRC is more efficient and stable when the torque disturbance happens as shown in Fig 6(a). What is more, Fig 6(b) shows that  $i_q$  has a smaller overshoot and faster dynamic response.



**Figure 6 : Dynamic response of ADRC based speed control under torque variations**

Case2: The simulation is conducted with a constant  $T_{mec} = 50N.m$ , and  $\omega^*$  changes from 150rad/s to 180rad/s at 0.1s. The speed tracking process of both controllers is almost the same as shown in Figure 8(a), but the overshoot of  $i_q$  is reduced with ADRC control as shown in Figure 8(b).

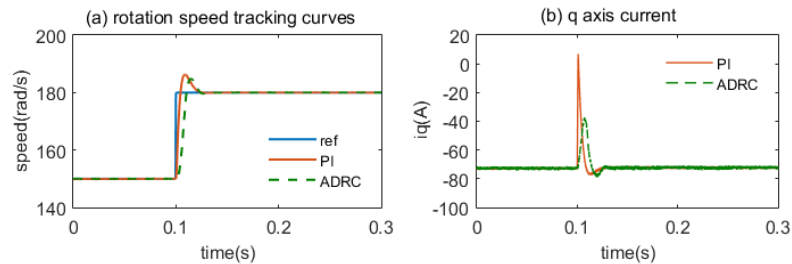


**Figure 6 : Dynamic response of ADRC based speed control under speed variations**

## 5.2 Experiment results

The experiments are conducted in a hardware-in-the-loop benchmark as shown in Figure 16 [2-4]. The hydro turbine model is computer-synthesized in the dSPACE hardware (DS1005), and its efficiency versus rotational speed for different values of water flow rates are saved in a look-up table. Then, the physical simulation of the hydro power operation is achieved by a torque-controlled direct current motor (DCM), the torque command of a DCM is generated through the MPPT control realized in dSPACE. The hydro turbine torque is generated in response to its real-time rotational speed such that it simulates the physical hydro turbine dynamic behavior in real time. The DCM control is implemented into a TMS320F240 digital signal processor. Finally, the PMSG is directly driven by the DCM, and the generator is connected to the power grid via back-to-back converters. The control algorithms of the variable speed system have been conducted with the same dSPACE hardware under MATLAB/Simulink environment.

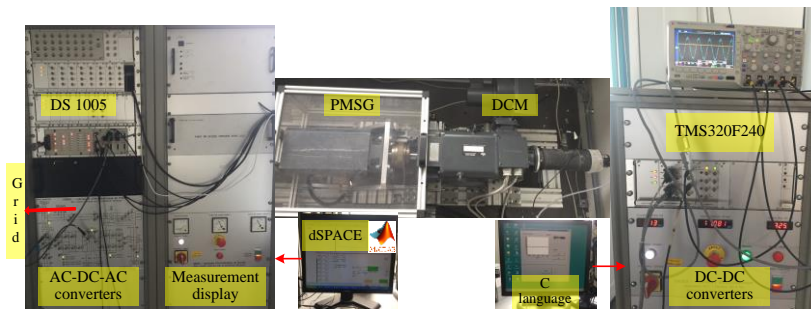


**Figure 9 : Hardware-in-the-loop experiment benchmark**

In the experiments, an adaptive MPPT technique proposed in [3] is employed. Moreover, to simulate the disturbances from the hydro turbine operation, a random fluctuation between 1N.m and -1N.m is manually injected to the hydro turbine torque. Figure 10 shows the performances of the ADRC based speed control. It can see the disturbances estimated change correspondingly with the speed variations, and then the influences of the disturbances are compensated in real time in the closed loop dynamics. The experiments results show the ADRC based speed control has fast dynamics and small steady state errors.

## 6. Conclusions

Micro-hydropower brings a significant contribution to the renewable energy section due to its huge potential through the world. A variable-speed operation has been widely used to realize the MPPT in MHPGSSs, and the hydro turbine rotation speed often changes with the water flow rates variations, which proposes higher demands for the speed control.

Furthermore, a MHPGS is a typical complex nonlinear system being disturbed by large unpredictable uncertainties. The ADRC technology, which can compensate the influences of the internal and the external disturbances in real time, is applied to the outer rotation speed control loop. The experiments results prove the ADRC based speed control has a fast transient response and small steady state errors, which realizes high-performance speed control.

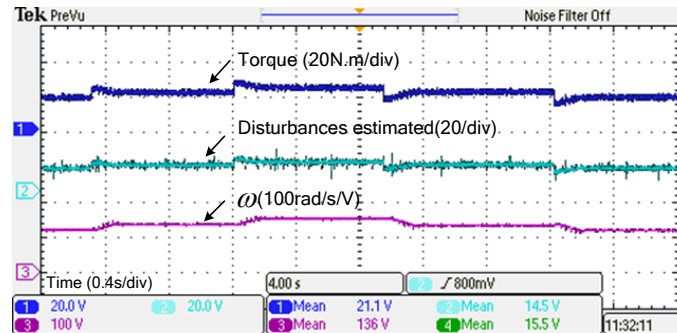


Figure 10 : Performance of the ADRC based speed control

## Acknowledgment

This paper is supported by PSPC Innov'hydro project, which specifically brings together GE Renewable, EDF, Grenoble INP and other key players in the hydroelectric sector, in France.

## Reference

- [1] World Small Hydropower Development Report 2016, published in 2016 by United Nations Industrial Development Organization and International Center on Small Hydro Power.
- [2] Belhadji, L., Bacha, S., & Roye, D. (2011, November). Modeling and control of variable-speed micro-hydropower plant based on axial-flow turbine and permanent magnet synchronous generator (MHPP-PMSG). In IECON 2011-37th Annual Conference on IEEE Industrial Electronics Society (pp. 896-901). IEEE.
- [3] Belhadji, L., Bacha, S., Munteanu, I., Rumeau, A., & Roye, D. (2013). Adaptive MPPT applied to variable-speed microhydropower plant. *IEEE Transactions on Energy Conversion*, 28(1), 34-43.
- [4] Belhadji, L., Bacha, S., Roye, D., & Rekioua, T. (2012, October). Experimental validation of direct power control of variable speed micro-hydropower plant. In IECON 2012-38th Annual Conference on IEEE Industrial Electronics Society (pp. 995-1000). IEEE.
- [5] Nababan, S., Muljadi, E., & Blaabjerg, F. (2012, June). An overview of power topologies for micro-hydro turbines. In *Power Electronics for Distributed Generation Systems (PEDG), 2012 3rd IEEE International Symposium on* (pp. 737-744). IEEE.
- [6] Shin, H., Jung, H. S., & Sul, S. K. (2011, May). Low voltage ride through (LVRT) control strategy of grid-connected variable speed Wind Turbine Generator System. In *Power Electronics and ECCE Asia (ICPE & ECCE), 2011 IEEE 8th International Conference on* (pp. 96-101). IEEE.
- [7] Marquez, J. L., Molina, M. G., & Pacas, J. M. (2010). Dynamic modeling, simulation and control design of an advanced micro-hydro power plant for distributed generation applications. *International journal of hydrogen energy*, 35(11), 5772-5777.
- [8] S. Kung and M. H. Tsai, "FPGA-Based Speed Control IC for PMSM Drive With Adaptive Fuzzy Control," in *IEEE Transactions on Power Electronics*, vol. 22, no. 6, pp. 2476-2486, Nov. 2007.
- [9] JUNG, Jin-Woo, LEU, Viet Quoc, DO, Ton Duc. Adaptive PID speed control design for permanent magnet synchronous motor drives. *IEEE Transactions on Power Electronics*, 2015, vol. 30, no 2, p. 900-908.
- [10] Han, J. (2009). From PID to active disturbance rejection control. *IEEE transactions on Industrial Electronics*, 56(3), 900-906.
- [11] Huang, Y., & Xue, W. (2014). Active disturbance rejection control: methodology and theoretical analysis. *ISA transactions*, 53(4), 963-976.
- [12] Zheng, Q., & Gao, Z. (2010, July). On practical applications of active disturbance rejection control. In *Control Conference (CCC), 2010 29th Chinese* (pp. 6095-6100). IEEE.
- [13] L. Wang, H. Zhang and X. Liu, "Robust sensorless of ADRC controlled PMSM based on MRAS with stator resistance identification," *Proceedings of the 30th Chinese Control Conference*, Yantai, 2011, pp. 3575-3579.
- [14] Z. Tong, G. Hong, X. Jinquan, K. Xiaolin and Q. Hao, "Research on PMSM active disturbance rejection controller based on model compensation," *2015 18th International Conference on Electrical Machines and Systems (ICEMS)*, Pattaya, 2015, pp. 1593-1596.
- [15] Zhigang and Li Shihua, "A Two-order Active Disturbance Rejection Control Algorithm for Permanent Magnetic Synchronous Motor," *2007 Chinese Control Conference*, Hunan, 2007, pp. 68-71.
- [16] Gao, Z. (2006, June). Scaling and bandwidth-parameterization based controller tuning. In *Proceedings of the American control conference* (Vol. 6, pp. 4989-4996).